



Flexural and impact behaviour of carbon/basalt fibers hybrid laminates

A Dorigato and A Pegoretti

Abstract

Basalt and E-glass fibers fabrics were combined with carbon fiber fabrics in order to prepare epoxy-based interlaminar hybrid composites and to investigate the hybridization effect on the flexural and impact properties of the resulting laminates. The flexural modulus of the composites depended on their composition according to a rule of mixture, while an important synergistic effect was detected for the ultimate flexural properties. Charpy impact tests evidenced a strength increase as basalt and glass fibers content increased. Interestingly, hybridization with basalt fibers promoted an increase of the adsorbed impact energy due to an enhancement of the fracture propagation component.

Keywords

Polymer-matrix composites, impact behaviour, laminate mechanics, mechanical testing

Introduction

Fiber-reinforced polymers (FRPs) offer several attractive features, including high mechanical performances, light weight and reduced lifecycle costs.¹ In the last decades, carbon fiber composites have become the dominant advanced composite materials for aerospace, automobile, sporting goods and other application due to their high strength, high modulus, good fatigue resistance, low density and elevated chemical stability. As the price of carbon fibers decreases, their applications have been broadened to the construction industry, which uses carbon to reinforce or repair concrete structures.² Due to their inherent brittleness, the main disadvantage related to the use of carbon fibers is the catastrophic mode of failure of the resulting composites.

A possible strategy to improve the fracture resistance of carbon fiber laminates is the combination with other types of reinforcing fibres, thus developing hybrid composite materials. In fact, in hybrid composites two or more types of fibers are simultaneously used as reinforcement. Although hybrid laminates may be produced in several different arrangements, in most cases fibers have been intimately mixed in a lamina (intraply hybrid laminates) or in separate laminae (interply hybrid laminates).³ In the past years, several efforts have been made to hybridize carbon fiber laminates by using various amounts of glass^{4–6} or aramid fibers.^{7–9} Although the mechanical properties of

hybrid laminates can be often modelled on the basis of the volume concentration of their constituents through the general rule of mixtures, many researchers revealed the existence of a hybrid effect in which the material property significantly differ from those predicted by the rule of mixtures.¹⁰

More recently, basalt fiber has been increasingly investigated as a possible substitute of traditional glass fibers in FRPs.^{11–13} Although basalt fibers can be produced starting from dark volcanic rocks, formed by solidified lava at different compositions,^{14–16} only certain types are suitable for the production of fibrous reinforcements. In particular, basalt rocks with SiO₂ content of about 46% (acid basalt) are required for fiber production. The manufacturing process of basalt filaments consists of melt preparation, fiber extrusion, application of sizing agents and final winding. Basalt fibers are characterized by density values in the range from 2.5 to 2.9 g cm⁻³, i.e. quite similar to that of glass fibers. As far as chemical resistance is concerned, basalt filaments present a superior resistance against alkaline environment with respect to glass fibers, while relatively less stability has been

Department of Industrial Engineering, University of Trento, Trento, Italy

Corresponding author:

A Dorigato, Department of Industrial Engineering, University of Trento, Via Mesiano 77, 38123 Trento, Italy.
Email: andrea.dorigato@ing.unitn.it

registered in strong acids.^{17–19} In the last decades, basalt fibers were extensively applied as geo-polymeric concretes,²⁰ pressure pipes,²¹ fibrous insulators,²² protective clothes^{20–24} and fire blocking material,^{15,25} and more recently as a reinforcement for polymer composites.^{26–39} For as the development of hybrid composites is concerned, basalt fibers were successfully combined with traditional reinforcements, such as glass,⁴⁰ carbon,^{41,42} aramid⁴³ and nylon⁴⁴ fibers. For instance, Cao et al. investigated the tensile properties of carbon fiber reinforced polymers (CFRP), hybrid carbon/glass and basalt/glass laminates subjected to temperatures ranging from 16 to 200°C.⁴¹ As the test temperature increased, hybrid laminates exhibited tensile strength values similar to CFRP sheets, but the dispersion of carbon tensile strengths in hybrid FRP was reduced compared to CFRP sheets, both by using glass and basalt reinforcements. Wu et al. investigated the fatigue behaviour of various fiber reinforced polymer (FRP) composites (carbon, glass, polyparaphenylenbenzobisoxazole (PBO) and basalt fibers), including the effect of hybrid applications such as carbon/glass and carbon/basalt composites.⁴² It was demonstrated how hybridization could reduce the dispersion of fatigue life of hybrid FRP sheets under the same maximum applied load, with an effect becoming more and more evident as the amounts of glass/basalt fibers increases. While the smooth surface of glass fibers resulted in a delamination failure mode between carbon and glass fiber sheets and in corresponding low fatigue resistance, the rough surface of basalt fibers could assure a good bond and a consequent enhancement of the fatigue resistance of the resulting laminates.

Apparently, no attention was devoted so far to the effect of the hybridization with basalt fibers on the impact behaviour of carbon fiber laminates. In a preliminary work of our group,⁴⁵ fabrics of basalt (BF), E-glass (GF) and carbon (CF) fibers with the same areal density were utilized to prepare epoxy-based laminates. Investigation of their tensile behaviour under fatigue conditions indicated superior performances of BF laminates with respect to the corresponding GF composites, with an improved capability of

sustaining progressive damaging and slightly higher damping properties. Taking into account the conclusions reported in that paper, the objective of the present work is to investigate the hybrid effect on the flexural and impact mechanical properties of epoxy-based carbon/basalt laminates. The presence of synergistic effects due to fiber hybridization and the role played by basalt reinforcements on the energy absorption mechanisms were evaluated and compared with the results obtained with the corresponding glass/basalt hybrids.

Experimental

Materials

A bi-component epoxy resin, supplied by Elantas Camattini (Collecchio, Italy), was used as polymer matrix. In particular, EC152 epoxy base (density of 1.15 g cm⁻³, viscosity of 1500 mPa s) and W152 LR aminic hardener (density of 0.95 g cm⁻³, viscosity of 30 mPa s) were mixed at a stoichiometric weight ratio of 100/30.

Carbon, basalt and E-glass bi-directional woven fabrics with the same areal density of 200 g m⁻², respectively denoted as C, B and G, were utilized. For as concerns the interlacement state, 2 × 2 twilled carbon fiber fabrics and plain basalt and E-glass fabrics were used. Carbon and glass fabrics were provided by Model Center – Urs Schaller S.a.s. (Florence, Italy), while basalt fabrics were furnished by Aldebran S.p.A. (Bergamo, Italy). The values of the density and the most important tensile properties of the matrix and of the fibers extracted from the fabrics, evaluated in a preliminary work on the same materials,⁴⁵ are summarized in Table 1.

Laminates preparation and characterization

Square laminates with a side of 300 mm were prepared by hand-lay up. Twenty impregnated fabric layers were stacked inside vacuum Mylar[®] bags and inserted between the flat metallic moulds of a 10-ton Carver

Table 1. Density, mean fiber diameter and quasi-static tensile properties of the polymer matrix and of the reinforcements utilized in this work.

Material	Density (g cm ⁻³)	Diameter (μm)	E (GPa)	σ _b (MPa)	ε _b (%)
Epoxy	1.14 ± 0.01	–	2.9 ± 0.1	70 ± 2	5.30 ± 1.00
C	1.73 ± 0.01	8.2 ± 0.4	201.0 ± 20.0	1526 ± 643	0.74 ± 0.27
G	2.62 ± 0.01	10.4 ± 0.6	69.0 ± 14.0	1035 ± 402	1.50 ± 0.46
B	2.59 ± 0.01	12.3 ± 1.1	64.0 ± 4.0	1586 ± 433	2.46 ± 0.68

E: elastic modulus; σ_b: tensile stress at break; ε_b: tensile strain at break.

Laboratory press. After degassing, a nominal pressure (i.e. referred to the composite plate surface) of 1 MPa was applied and the laminates were cured under pressure and vacuum for 2 h at 50°C and 2 h at 80°C. In this way, composite laminates reinforced with carbon, glass and basalt fibers were prepared, together with the corresponding hybrid laminates at different relative compositions. Samples were designated indicating the type of matrix (Epoxy), followed by the kind of reinforcement and the number of plies in the laminates. As an example, Epoxy + C denotes the composite laminate reinforced with carbon fibers, while Epoxy + G10C10 indicates the hybrid laminate with 10 plies of glass fibers and 10 plies of carbon fibers. Table 2 summarizes the prepared laminates with their stacking sequence.

The total fiber weight percentage in the laminates ($W_{f,TOT}$) was determined through thermogravimetric analyses (TGA) performed by a Mettler TG50 apparatus from 30°C to 700°C, at a heating rate of 10°C min⁻¹ under a nitrogen flow of 20 mL min⁻¹. At least three specimens with a mass of about 50 mg were tested for each sample. The effective fiber weight fraction in the composites was determined by subtracting from the mass residue at 700°C the char content due to matrix degradation, that was previously determined by separate TGA tests on neat epoxy matrix. The weight fraction of the various fibers in the composites ($W_{f,C}$, $W_{f,G}$, $W_{f,B}$) can be estimated by knowing the areal density (g_C , g_G , g_B) and the number of the plies in the laminates (N_C , N_G , N_B). The theoretical density of the composites ($\rho_{c,th}$) can therefore be determined with the following relation:

$$\rho_{c,th} = \frac{1}{\frac{W_m}{\rho_m} + \frac{W_{f,B(G)}}{\rho_{B(G)}} + \frac{W_{f,C}}{\rho_C}} \quad (1)$$

The overall fiber volume percentage in the laminates ($\phi_{f,TOT}$) can be determined as follows:

$$\phi_{f,TOT} = 100 - \frac{\rho_{c,th}}{\rho_m} W_m \quad (2)$$

while the void volume fraction in the composites (ϕ_V) was determined as:

$$\phi_V = \frac{\rho_{c,th} - \rho_{c,exp}}{\rho_{c,th}} \quad (3)$$

where the experimental density of the composites ($\rho_{c,exp}$) was assessed by the buoyancy method (i.e. Archimedes principle) in ethanol (Sigma Aldrich, 98% purity) according to ASTM D792 standard. Starting from the knowledge of $\phi_{f,TOT}$, the relative volume fraction of the various fibers in the hybrid laminates ($\phi_{f,C}$, $\phi_{f,G}$, $\phi_{f,B}$) can be derived in the following way:

$$\frac{\phi_{f,C}}{\phi_{f,G(B)}} = \frac{g_C \cdot N_C}{\rho_{f,C}} \cdot \frac{\rho_{f,G(B)}}{g_{G(B)} \cdot N_{G(B)}} \quad (4)$$

$$\phi_{f,TOT} = \phi_{f,C} + \phi_{f,G(B)} \quad (5)$$

Three point flexure tests were performed by using an Instron 4502 universal testing machine, equipped with a 10 kN load cell. Rectangular specimens having a thickness (d) of 3 mm, a width (b) of 8 mm and a span length (L) of 95.5 mm were tested. According to ASTM 790 standard, all tests were performed setting a crosshead speed of 5 mm min⁻¹, corresponding to a strain rate in the outer part of middle section equal to 0.01 min⁻¹. At least ten specimens were tested for each sample. In this way it was possible to determine the flexural modulus (E_f), the maximum flexural stress ($\sigma_{max,f}$) and the maximum flexural strain ($\varepsilon_{max,f}$) of the tested specimens.

Short beam shear strength tests were performed by using the same universal testing machine utilized in flexural tests, at a crosshead speed of 1 mm min⁻¹. According to ASTM D2344 standard, these tests were carried out on rectangular samples having a span length of 12 mm, with a span length/thickness ratio of 4. At least ten specimens for each sample were tested. In this

Table 2. List of the prepared laminates with the corresponding stacking sequence.

Laminate code	Number of laminae	Stacking sequence	Thickness (mm)
Epoxy + C	20	[C] ₂₀	3.18 ± 0.11
Epoxy + G	20	[G] ₂₀	3.12 ± 0.02
Epoxy + B	20	[B] ₂₀	3.02 ± 0.01
Epoxy + G10C10	10 (G) + 10 (C)	[G/C/G/C/G/C/G/C/G/C] ₅	2.91 ± 0.01
Epoxy + B10C10	10 (B) + 10 (C)	[B/C/B/C/B/C/B/C/B/C] ₅	2.84 ± 0.01
Epoxy + G6C14	6 (G) + 14 (C)	[C/C/G/C/C/G/C/C/G/C/C] ₅	2.99 ± 0.03
Epoxy + B6C14	6 (B) + 14 (C)	[C/C/B/C/C/B/C/C/B/C] ₅	2.94 ± 0.01
Epoxy + G14C6	14 (G) + 6 (C)	[G/G/C/G/G/C/G/G/C/G] ₅	2.74 ± 0.03
Epoxy + B14C6	14 (B) + 6 (C)	[B/B/C/B/B/C/B/B/C/B] ₅	2.75 ± 0.01

way, the influence of fiber hybridization on the interlaminar shear strength (ILSS) of the tested laminates was determined.

Charpy impact tests were performed by using a Ceast instrumented impact pendulum on specimens having the same size of those utilized in flexural tests. Tests were performed according to ASTM D6110 standard, by using a striker mass of 8.36 kg, an initial impact angle of 87° and an acquisition rate of 2000 Hz. In this way, samples were impacted at a speed of 2.16 ms⁻¹. At least five specimens were tested for each sample. The maximum impact stress ($\sigma_{\max,f}$) was evaluated according to the following equation:

$$\sigma_{\max,f} = \frac{3FL}{2bd^2} \left[1 + 6 \left(\frac{\delta}{L} \right)^2 - 4 \left(\frac{d}{L} \right) \left(\frac{\delta}{L} \right) \right] \quad (6)$$

where F and δ respectively represent the maximum force and the deflection at the maximum force. Through the integration of force-displacement curves it was therefore possible to evaluate the specific energy adsorbed at fracture initiation (E_i), corresponding to the energy adsorbed up to the maximum load, the propagation (E_P) and the total (E_{TOT}) amount of the adsorbed specific energy, where $E_{\text{TOT}} = E_i + E_P$. The ductility index (DI), defined as the ratio between E_P and E_i , was utilized to determine the energy absorption capability of the tested laminates during damage propagation.⁴⁶

Results and discussion

Flexural test

Density, total fiber content, volume fractions of the various types of reinforcements and void volume fraction of the investigated laminates are summarized in

Table 3. First of all, it is worthwhile to observe that the total fiber content in the laminates hybridized with basalt fibers is slightly higher than that reported for the corresponding carbon/glass laminates. Considering that the utilized glass and basalt fabrics have the same areal density, these slight discrepancies can be attributed to a better wetting capability of basalt fabrics. However, for all the tested laminates $\phi_{f,\text{TOT}}$ values lie in the interval 50–65%, that is a common range for the fiber loading of composite laminates prepared through hand lay-up technique. Moreover, the differences in $\phi_{f,\text{TOT}}$ values between hybrid laminates with the same G/C and B/C ratio are lower than 6%. The investigated laminates are in general comparable also for as the void content is concerned, that is generally lower than 4%. Only for the Epoxy + G6C14 sample an higher ϕ_V value was determined (6.94%). It can be therefore concluded that the mechanical properties of these laminates are directly comparable, at least from a qualitative point of view.

In Figure 1, representative curves of the quasi-static flexural tests on the single fiber composites and of the relative hybrid laminates are represented, while in Figure 2(a)–(c), the most important flexural properties are plotted as a function of the relative carbon fiber volume content. In these figures, experimental results are compared with theoretical predictions obtained through the application of the rule of mixtures. It is important to underline that these calculations are based on the experimental results at 0 and 1.0 relative carbon fraction and do not consider the contributions of the fibres and resin matrix as separate components. As expected, the force-displacement plot of the Epoxy + C laminate is characterized by an elevated flexural modulus and maximum stress and limited strain at failure. As expected, neat basalt and glass fiber laminates are characterized by lower stiffness, but similar flexural strength with respect to the

Table 3. Density, total fiber volume fraction ($\phi_{f,\text{TOT}}$), carbon (ϕ_{fC}), basalt (ϕ_{fB}) and glass (ϕ_{fG}) fiber volume content, and void content (ϕ_V) of the investigated laminates.

Laminate code	Density (g cm ⁻³)	$\phi_{f,\text{TOT}}$ (%)	ϕ_{fC} (%)	ϕ_{fB} (%)	ϕ_{fG} (%)	ϕ_V (%)
Epoxy + G	1.81 ± 0.01	50.0	–	–	50.0	3.57
Epoxy + B	1.90 ± 0.01	55.4	–	55.4	–	2.70
Epoxy + C	1.46 ± 0.02	65.5	65.5	–	–	4.20
Epoxy + B6C14	1.66 ± 0.01	66.5	51.1	15.4	–	2.82
Epoxy + G6C14	1.65 ± 0.01	60.5	46.6	–	13.9	6.94
Epoxy + B10C10	1.73 ± 0.01	65.8	38.7	27.1	–	3.64
Epoxy + G10C10	1.73 ± 0.02	62.1	36.6	–	25.5	3.83
Epoxy + B14C6	1.84 ± 0.01	64.3	24.4	39.9	–	2.22
Epoxy + G14C6	1.84 ± 0.01	61.5	23.4	–	38.1	1.84

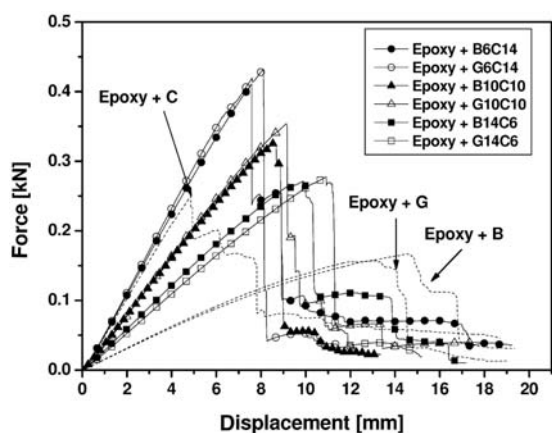


Figure 1. Representative curves of the quasi-static flexural tests on the neat composites (dotted lines), on basalt/carbon fiber (full symbols) and on glass/carbon fiber (open symbols) hybrid laminates.

corresponding carbon fiber laminate, and higher strain at break values. From Figure 2(a), it can be inferred that flexural moduli of the hybrid laminates are in good accordance with theoretical predictions based on the rule of mixture (solid line). Interestingly enough, Figure 2(b) and (c) highlight how hybridization with glass or basalt fibers promotes a remarkable synergistic effect both on the flexural strength and, to a lower extent, on the maximum flexural strain. The highest deviation from theoretical predictions of the rule of mixture can be obtained with a relative carbon content of 75%, both by considering basalt and glass reinforcements. Considering the standard deviation values associated to each measurement, it can be concluded that the effect produced by the introduction of basalt fibers in the investigated laminates is very similar to that obtained introducing glass fiber fabrics at the same relative amount. A positive hybrid effect due to the addition of glass fibers in carbon/epoxy composites is well documented in the scientific literature, its

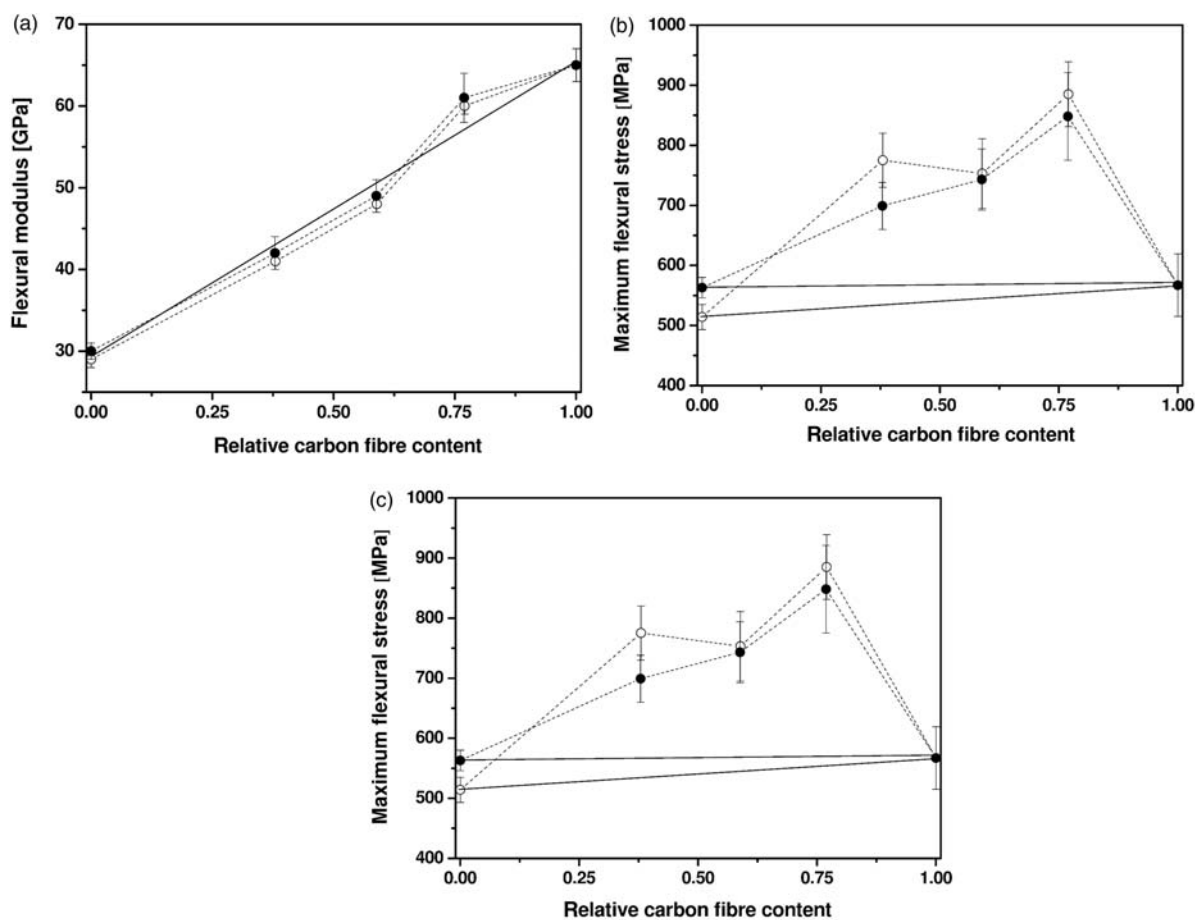


Figure 2. Results of the flexural tests on basalt/carbon fiber (full symbols) and on glass/carbon fiber (open symbols) hybrid laminates, with the fitting line according to the rule of mixture (full line). (a) Flexural modulus, (b) flexural strength and (c) maximum strain at break (the relative carbon fiber content was taken from Table 3).

extent being dependent on the ratio of the two fibre types, upon their dispersion and on the quality of the interfaces involved.^{5,6,8,10,47–52} In particular, positive deviations from the rule of mixture have been reported for various mechanical parameters, such as the failure strain,^{5,6} fracture behaviour,⁵² impact resistance^{48–50} and fatigue behaviour.^{8,47} More recently, Dong et al. investigated the flexural properties of S-2 glass and carbon fiber-reinforced epoxy hybrid composites.⁵³ In this work, a partial substitution of carbon fiber with S-2 glass fibers resulted in a noticeable increase of the flexural strength of the resulting composites. In particular, a positive deviation of more than 70% with respect to the value theoretically predicted with the rule of mixture was observed for an S-2 glass fiber percentage of about 40% of the total fiber volume fraction. The flexural behavior was also simulated by finite element analysis (FEA). Based on the FEA results, the flexural modulus and flexural strength were calculated. Good agreement was found between the experiments and FEA. These observations are in partial agreement with a study by Sudarisman et al.,⁵⁴ who reported a positive hybrid effect on the flexural strength with smaller amounts of glass fiber substitution (approximately up to 25%) in a glass/carbon composite.⁵⁴ Even if an exhaustive explanation was not provided by the above-mentioned authors, the unusual high flexural strength values were associated to the occurrence of a certain delamination.

An examination of the existing literature on the subject provide some possible explanation of the so called “hybrid effect.” The occurrence of an hybrid effect has been partly attributed to the internal compressive strains induced in the carbon phase by differential thermal contraction as the composite is cooled from its cure temperature.^{5,6} Another possible explanation for the observed hybrid effect is based on the crack-constraint theory of hybrid composites.^{55,56} When loading a hybrid composite, carbon fibers will first begin to fracture. At the same time, glass (or basalt) fibers around the carbon fibers will prevent the cracks in the carbon fibers from spreading, which can carry the load released by fracture of the carbon fibers. As a result, carbon fiber reinforced composites with the hybridization of glass or basalt fibers may have higher tensile strength and higher rupture strain than single carbon fiber composites. However, a more detailed investigation on the fracture mechanism on these systems will be required in the future to find an exhaustive explanation for the obtained results. In particular, fracture surface micrographs could give more information about the microstructural effects associated to the observed hybrid effect.

In order to have a better comprehension of the role played by fiber hybridization on the mechanical

properties of the prepared composites, the interlaminar adhesion level has been evaluated through short beam shear tests. In Table 4, ILSS values of the investigated laminates are summarized. ILSS values of the composites reinforced with glass and basalt fibres are very similar and close to about 60 MPa. On the other hand, the ILSS value of carbon/epoxy composites is slightly lower and equal to 55.7 MPa. Interestingly, ILSS values of hybrid laminates are systematically lower than that of the neat composites. In all cases, the fracture surface was located in the middle plane of the laminate, where the shear stress reaches its maximum intensity. The behaviour of hybrid laminates is strictly related to the type of laminae involved in the delamination process. In fact, for Epoxy + B6C14, Epoxy + G6C14, Epoxy + B10C10 and Epoxy + G10C10 samples, the delamination is located between two carbon/epoxy laminae and, consequently, ILSS values are lower than those observed for Epoxy + B14C6 and Epoxy + G14C6 samples, for which the delamination occurs between basalt/epoxy and glass/epoxy laminae, respectively.

Impact test

Representative force-displacement curves of the Charpy impact tests on the neat laminates and the relative hybrid composites are represented in Figure 3(a)–(c). As often reported in literature, Epoxy + C laminate is characterized by a relatively brittle behaviour, with elevated maximum force values and a relatively low-energy absorption capability both during fracture initiation and propagation stages. Even in this case, neat basalt and glass fiber composites show a similar behaviour, with a superior absorption capability with respect to carbon fiber laminates. The most important results obtained from the impact tests are reported in Figure 4(a)–(d) as a function of the

Table 4. Interlaminar shear strength (ILSS) values of the investigated laminates.

Laminate code	ILSS (MPa)
Epoxy + G	59.7 ± 1.4
Epoxy + B	60.2 ± 0.9
Epoxy + C	55.7 ± 2.1
Epoxy + B6C14	45.2 ± 0.9
Epoxy + G6C14	43.5 ± 1.3
Epoxy + B10C10	46.9 ± 0.6
Epoxy + G10C10	45.9 ± 2.0
Epoxy + B14C6	53.2 ± 1.0
Epoxy + G14C6	54.0 ± 0.5

relative carbon fiber content, and compared with the theoretical predictions according to the rule of mixture. Even in this case, theoretical calculations are based on the experimental results at 0 and 1.0 relative carbon fraction and do not take into account the separate contributions of the fibres and resin matrix. In accordance with the results reported for flexural test, Figure 4(a) evidences how hybridization with both basalt and glass fibers induces a pronounced synergistic effect on the maximum impact stress, with a positive deviation with respect to theoretical values obtained according to the rule of mixture. Even in this case, the best results are obtained at a relative carbon fiber content of 75%. Considering the data dispersion (quantified by error bars in Figure 4) associated to this parameter, it can be concluded that also in this case glass and basalt fibers present a similar behaviour. Once again, the increase in the flexural strength under impact conditions observed for the hybrid laminates with respect to the predictions of the rule of mixture could be attributed to the crack-constraint effect provided by basalt and glass fibers on the broken carbon fibers. For as

concerns energy absorption capability, Figure 4(b) indicates that the experimental values of the specific energy absorbed at fracture initiation (E_i) substantially follow the rule of mixture, with a progressive decrease of E_i values as the relative carbon fiber content increases. More interesting results can be obtained considering the energy absorption during the fracture propagation stage (E_p). In fact, Figure 4(c) highlights how for both basalt/carbon and glass/carbon fiber hybrid composites the trends of E_p values display a positive deviation from the rule of mixture represented by the solid lines. This hybrid effect is particularly pronounced for when carbon fibers are replaced by basalt fiber at a relative amount of 40%. As documented in Figure 4(d), the ductility index values of basalt/carbon hybrids are higher than that of glass/carbon hybrids at the same relative concentration. It can be therefore concluded that basalt fibers are more efficient than glass fibers in increasing the energy absorption capability during the damage propagation stages. In a previous paper of our group,⁴⁵ it was demonstrated how specific damping capacity (SDC) under fatigue loading of neat basalt

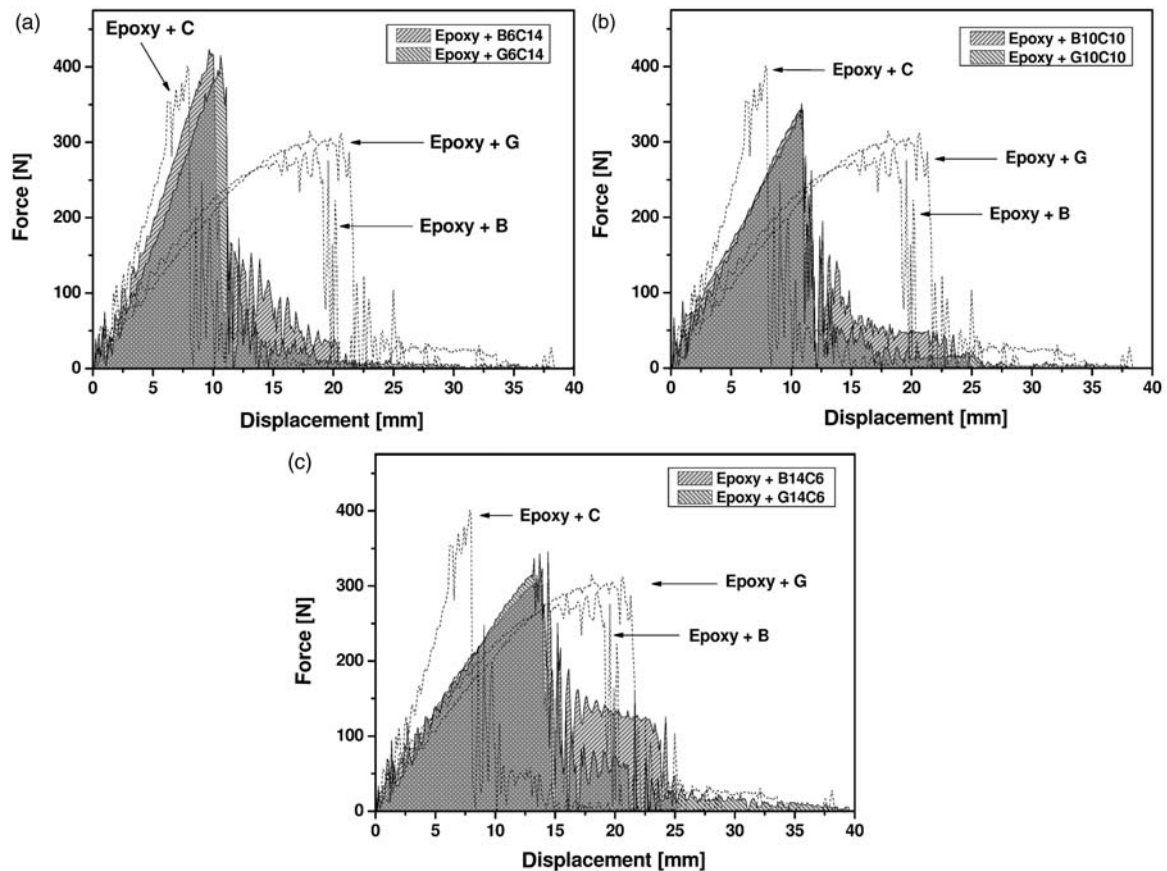


Figure 3. Representative curves of the Charpy impact tests on (a) Epoxy + B6C14 and Epoxy + G6C14, (b) Epoxy + B10C10 and Epoxy + G10C10, (c) Epoxy + B14C6 and Epoxy + G14C6 hybrid laminates. Experimental data of the neat laminates are represented with dotted lines.

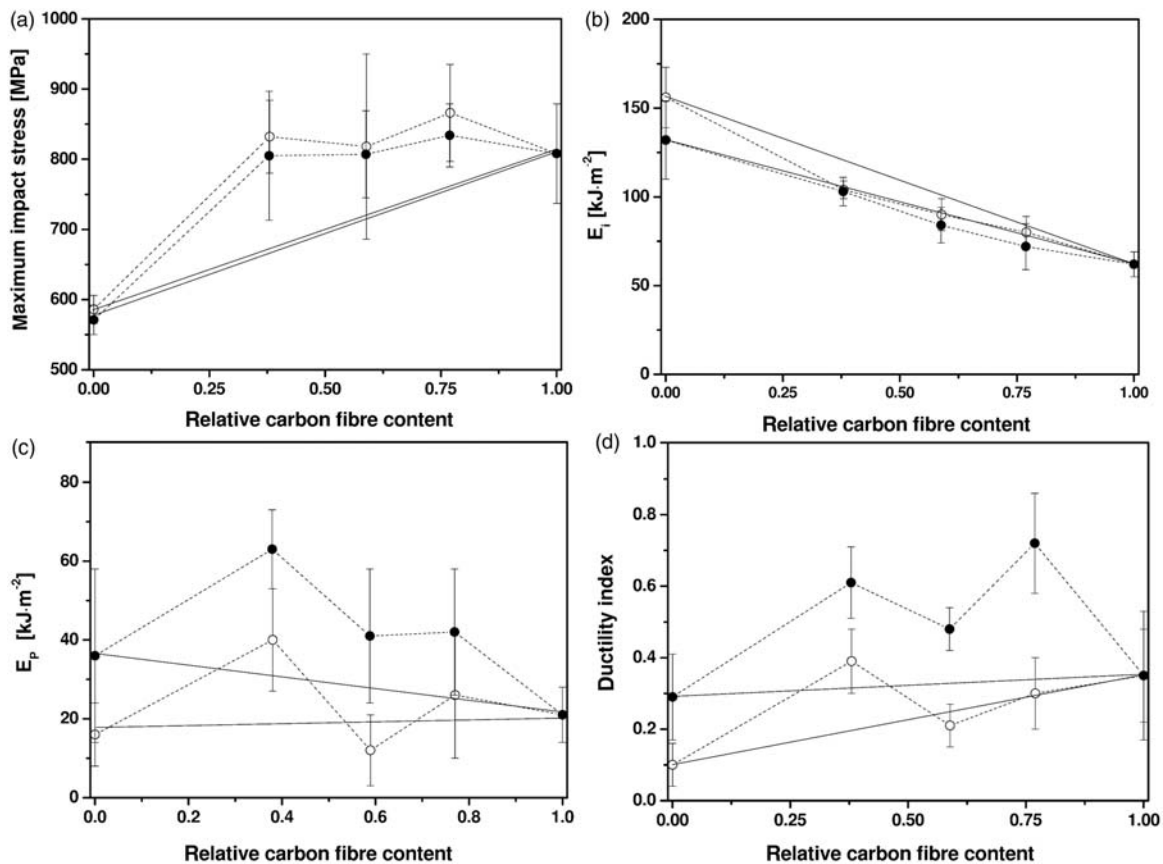


Figure 4. Results of the Charpy impact tests on basalt/carbon fiber (full symbols) and on glass/carbon fiber (open symbols) hybrid laminates, with the fitting line according to the rule of mixture (full line). (a) Impact strength, (b) specific energy to fracture initiation, (c) total adsorbed specific energy and (d) ductility index (the relative carbon fiber content was taken from Table 3).

fiber laminates was higher than that of the corresponding glass fiber composites. Moreover, the observed improvement in the damping capacity of basalt fiber laminates was correlated to the drop of the tensile modulus experienced at elevated fatigue loads. In that paper, it was hypothesized that the increase in damping capability of basalt fiber laminates could be associated to an increase of the crack density developing in the material during the fatigue test. Therefore, the higher DI values experienced in the present work upon basalt fiber hybridization could be probably related to the improved ability of basalt/carbon laminates to sustain crack propagation and delamination without catastrophic failure.

Conclusions

Epoxy-based hybrid laminates were prepared combining BF and GF in CF laminates at different relative amounts and mechanically characterized under flexural and impact conditions. Flexural moduli of the hybrid composites followed the rule of mixture, while positive deviations with important synergistic effects were

detected for the ultimate properties. Charpy impact tests confirmed the synergistic effects on the maximum strength upon glass and basalt fiber hybridization. Moreover, the introduction of basalt fibers in the carbon fiber laminates could promote an increase of the adsorbed impact energy, with an enhancement of the fracture propagation component. The observed improvements were related to the improved capability of basalt/carbon laminates in sustaining the damage propagation and delamination without catastrophic failure.

Acknowledgements

Mr. Andrea Debortoli is gratefully acknowledged for his support to the experimental work.

Conflict of Interest

None declared.

Funding

This research received no specific grant from any funding agency in the public, commercial, or not-for-profit sectors.

References

1. Gay D, Hoa SV and Tsai SW. *Composite materials. Design and applications*. Boca Raton, FL: CRC Press, 2003.
2. Chung DDL. *Carbon fiber composites*. Newton, MA, USA: Butterworth-Heinemann, 1994.
3. Pegoretti A, Fabbri E, Migliaresi C, et al. Intraply and interply hybrid composites based on E-glass and poly(vinyl alcohol) woven fabrics: tensile and impact properties. *Polym Int* 2004; 53: 1290–1297.
4. Bunsell A and Harris B. Hybrid carbon and glass fibre composites. *Composites* 1974; 5: 157–164.
5. Manders P and Bader G. The strength of hybrid glass/carbon fibre composites. Part 1. Failure strain enhancement and failure mode. *J Mater Sci* 1981; 16: 2233–2245.
6. Manders P and Bader G. The strength of hybrid glass/carbon fibre composites. Part 2. A statistical model. *J Mater Sci* 1981; 16: 2246–2256.
7. Aronhime J, Harel H, Gilbert A, et al. The rate-dependence of flexural shear fatigue and uniaxial compression of carbon-fiber and aramid-fiber composites and hybrids. *Compos Sci Technol* 1992; 43: 105–116.
8. Marom G, Harel H, Neumann S, et al. Fatigue behaviour and rate-dependent properties of aramid fiber carbon-fiber hybrid composites. *Composites* 1989; 20: 537–544.
9. Schulte K, Peters PWM and Chou TW. Hardness conditions in hybrid laminates with carbon-fibers and aramid fibers in comparison with pure carbon-fiber and aramid fiber textile laminates. *Kautschuk Gummi Kunststoffe* 1985; 38: 59–59.
10. Marom G, Fischer A, Tuler F, et al. Hybrid effects in composites: conditions for positive or negative effects versus rule-of-mixture behaviour. *J Mater Sci* 1978; 13: 1479–1426.
11. Czigany T. Trends in fiber reinforcements - the future belongs to basalt fiber. *Expr Pol Lett* 2007; 1: 59–59.
12. De Rosa IM, Marra F, Pulci G, et al. Post-impact mechanical characterisation of E-glass/basalt woven fabric interply hybrid laminates. *Expr Pol Lett* 2011; 5: 449–459.
13. Bashar M, Sundararaj U and Mertiny P. Study of matrix micro-cracking in nano clay and acrylic tri-block-copolymer modified epoxy/basalt fiber-reinforced pressure-retaining structures. *Expr Pol Lett* 2011; 5: 882–896.
14. Vladimir K and Vladimir L. Fibres from stone. *Int Text Bull* 2003; 5: 48–52.
15. Nolf JM. Basalt Fibres - Fire Blocking Textiles. *Tech Usage Text* 2003; 49: 38–42.
16. Saravanan D. Spinning the rocks - basalt fibres. *IE(I) J-TX* 2006; 86: 39–45.
17. Milman SB, Velikanova MG and Kotov LE. Development and study of load bearing heat insulation. *Cryogenics* 1996; 36: 127–130.
18. Wei B, Cao HL and Song SH. Environmental resistance and mechanical performance of basalt and glass fibers. *Mater Sci Eng A* 2010; 527: 4708–4715.
19. Subramanian RV and Austin HF. Silane coupling agents in basalt-reinforced polyester composites. *Int J Adhes Adhes* 1980; 1: 50–54.
20. Dias DP and Thaumaturgo C. Fracture toughness of geopolymeric concretes reinforced with basalt fibres. *Cem Concr Compos* 2005; 27: 49–54.
21. Hansen T. Basalt lined ash pipe still in service after nearly four decades. *Power Eng* 2005; 109: 70–71.
22. Novitskii AG and Sudakov VV. An unwoven basalt-fibre material for the encasing of fibrous insulation: an alternative to glass cloth. *Refract Ind Ceram* 2004; 45: 234–241.
23. Tropina LV, Vasyhk CG, Korniyushina VL, et al. New cloth from basalt fibres. *Fibre Chem* 1995; 27: 67–68.
24. Sezemanas G, Keriene J, Sinica M, et al. The alkali and temperature resistance of some fibres. *Mater Sci* 2005; 11: 29–35.
25. Landucci G, Rossi F, Nicoletta C, et al. Design and testing of innovative materials for passive fire protection. *Fire Safety J* 2009; 44: 1103–1109.
26. Artemenko SE. Polymer composite materials made from carbon, basalt, and glass fibres. Structure and properties. *Fibre Chem* 2003; 35: 226–229.
27. Artemenko SE and Kadykova YA. Polymer composite materials based on carbon, basalt, and glass fibres. *Fibre Chem* 2008; 40: 37–39.
28. Carmisciano S, De Rosa IM, Sarasini F, et al. Basalt woven fiber reinforced vinylester composites: Flexural and electrical properties. *Mater Des* 2011; 32: 337–342.
29. Colombo C, Vergani L and Burman M. Static and fatigue characterisation of new basalt fibre reinforced composites. *Compos Struct* 2012; 94: 1165–1174.
30. Czigany T, Poloskei K and Karger-Kocsis J. Fracture and failure behavior of basalt fiber mat-reinforced vinylester/epoxy hybrid resins as a function of resin composition and fiber surface treatment. *J Mater Sci* 2005; 40: 5609–5618.
31. Dalinkevich AA, Gumargalieva KZ, Marakhovskiy SS, et al. Modern basalt fibrous materials and basalt fiber-based polymeric composites. *J Nat Fibers* 2009; 6: 248–271.
32. Deak T, Czigany T, Marsalkova M, et al. Manufacturing and testing of long basalt fiber reinforced thermoplastic matrix composites. *Polym Eng Sci* 2010; 50: 2448–2456.
33. Kracalik M, Pospisil L, Slouf M, et al. Recycled poly(ethylene terephthalate) reinforced with basalt fibres: Rheology, structure, and utility properties. *Polym Compos* 2008; 29: 437–442.
34. Li WD, Cao HL, Chen GR, et al. Preparation and characterization of BF reinforced phenolic resin-based composites. *J Adv Mater* 2010; 42: 67–73.
35. Liu Q, Shaw MT, Parnas RS, et al. Investigation of basalt fiber composite mechanical properties for applications in transportation. *Polym Compos* 2006; 27: 41–48.
36. Lopresto V, Leone C and De Iorio I. Mechanical characterisation of basalt fibre reinforced plastic. *Composites Part B* 2011; 42: 717–723.
37. Pakharenko VV, Yanchar I, Pakharenko VA, et al. Polymer composite materials with fibrous and disperse basalt fillers. *Fibre Chem* 2008; 40: 246–252.
38. Sergeev VP, Chuvashov YN, Galushchak OV, et al. Basalt fibers. A reinforcing filler for composites. *Powder Metall Met Ceram* 1994; 33: 555–557.

39. Ozturk S. The effect of fibre content on the mechanical properties of hemp and basalt fibre reinforced phenol formaldehyde composites. *J Mater Sci* 2005; 40: 4585–4592.
40. De Rosa I, Marra F, Pulci G, et al. Post-impact mechanical characterisation of E-glass/basalt woven fabric interply hybrid laminates. *Expr Pol Lett* 2011; 5: 449–459.
41. Cao SH, Wu ZS and Wang X. Tensile properties of CFRP and hybrid FRP composites at elevated temperatures. *J Compos Mater* 2009; 43: 315–330.
42. Wu Z, Wang X, Iwashita K, et al. Tensile fatigue behaviour of FRP and hybrid FRP sheets. *Composites Part B* 2010; 41: 396–402.
43. Wang X, Hu B, Feng Y, et al. Low velocity impact properties of 3D woven basalt/aramid hybrid composites. *Compos Sci Technol* 2008; 68: 444–450.
44. Dehkordi MT, Nosraty H, Shokrieh MM, et al. Low velocity impact properties of intra-ply hybrid composites based on basalt and nylon woven fabrics. *Mater Des* 2010; 31: 3835–3844.
45. Dorigato A and Pegoretti A. Fatigue resistance of basalt fibres-reinforced laminates. *J Compos Mater* 2012; 46: 1773–1785.
46. Agarwal B and Broutman L. *Analysis and performance of fiber composites*. New York, USA: John Wiley and Sons, 1990.
47. Dickson RF, Fernando G, Adam T, et al. Fatigue behavior of hybrid composites. Part 2. Carbon-glass hybrids. *J Mater Sci* 1989; 24: 227–233.
48. Enfedaque A, Molina-Aldareguia JM, Galvez F, et al. Effect of glass fiber hybridization on the behavior under impact of woven carbon fiber/epoxy laminates. *J Compos Mater* 2010; 44: 3051–3068.
49. Naik NK, Ramasimha R, Arya H, et al. Impact response and damage tolerance characteristics of glass-carbon/epoxy hybrid composite plates. *Compos Part B* 2001; 32: 565–574.
50. Sayer M, Bektas NB, Sayman O, et al. An experimental investigation on the impact behaviour of glass/epoxy and hybrid composite plates. *Adv Compos Lett* 2009; 18: 113–122.
51. Stevanovic MM and Stecenko TB. Mechanical behavior of carbon and glass hybrid fiber reinforced polyester composites. *J Mater Sci* 1992; 27: 941–946.
52. Thorat HT and Lakkad SC. Fracture toughness of unidirectional glass carbon hybrid composites. *J Compos Mater* 1983; 17: 2–14.
53. Dong CS, Duong J and Davies IJ. Flexural properties of S-2 glass and TR30S carbon fiber-reinforced epoxy hybrid composites. *Polym Compos* 2012; 33: 773–781.
54. Sudarisman, de San Miguel B and Davies I, *The effect of partial substitution of E-glass fibre for carbon fibre on the mechanical properties of CFRP composites*. In: *International Conference on Materials and Metallurgical Technology 2009 (ICOMMET 2009)*. 2009: Surabaya, Indonesia, pp.125–128.
55. Song H and Zhang Z. *Properties of unidirectional hybrid composites, hybrid fiber composites*. Beijing: Beijing University of Aeronautics and Astronautics Press, 1988.
56. Wu Z, Sakamoto K, Iwashita K, et al. Hybridization of continuous fiber sheets as structural composites. *Jpn Soc Compos Mater* 2006; 32: 12–21.